

BEHAVIOUR OF DUCTILE MATERIALS UNDER IMPULSIVE LOADING

By

Dr. M.Y. Brunner
Department of Civil Engineering
University of Dar es Salaam

ABSTRACT

Ductile materials under dynamic loading are known to be able to absorb energy and thereby delay or even prevent structural failure. This paper is concerned with such behaviour in the case of impulsive loads of short duration. It is shown that even when the feared, unstable, labile condition is attained, failure may not necessarily occur. This behaviour is particularly impressive for structures with large mass, because it is essentially the mass which slows down the attainment of the failure strains. If the impulsive load dies away quickly enough, the constant plastic resistance will be adequate to bring the increasing deformations to a halt, thus preventing failure. The theoretical considerations are backed up by large-scale loading experiments.

1. INTRODUCTION

1 INTRODUCTION

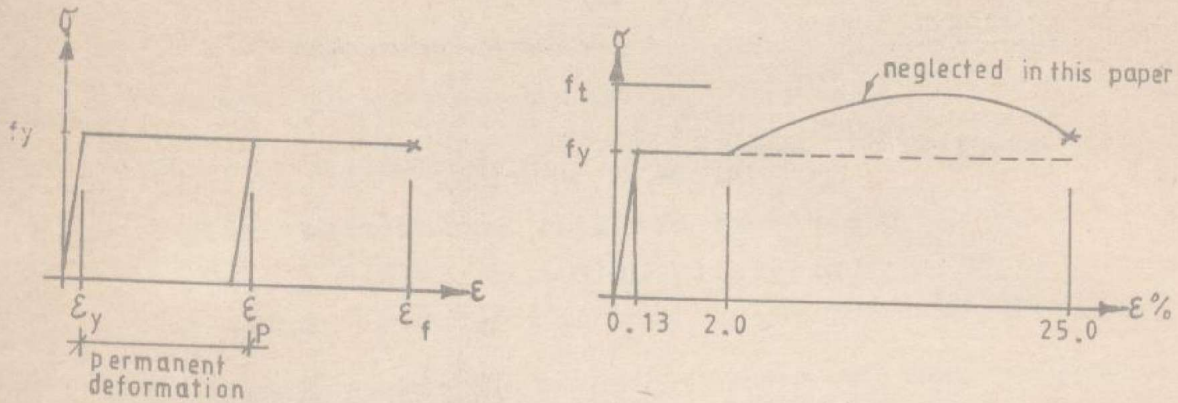


Fig. 1: Elasto plastic behaviour; a) simplified; b) Actual values for a typical construction on steel

Fig.1: Elasto-plastic behaviour: (a) simplified; (b) actual values for a typical construction steel.

Many typical building materials exhibit elasto-plastic behaviour (fig. 1). In the case of steel for example the ductility factor r which is defined as:

$$r = \frac{\text{Strain where failure occurs}}{\text{Strain where yielding begins}} = \frac{\epsilon_f}{\epsilon_y}$$

generally exceeds 16.

Structural engineers appreciate ductility, for example in the plastic analysis of statically indeterminate systems, whereby plastic joints develop in stages: collapse finally occurs only when the unstable or "labile" state is attained (fig.2).

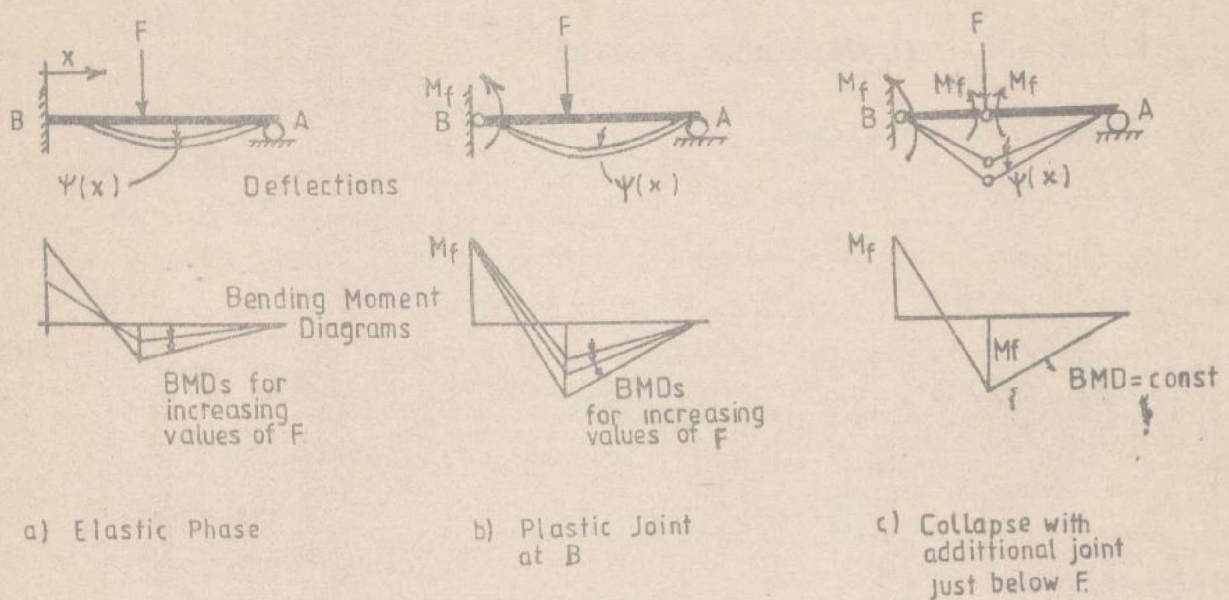


Figure 2: Elasto-plastic behaviour of a Beam.

In the case of long-duration loads, the attainment of the labile state will invariably lead to collapse. In the case of short duration impulsive loads, however, the attainment of the labile state may not necessarily lead to failure. The reason lies in the time interval between the attainment of the yield strain and the failure strain (see fig. 1a), which, particularly for heavy structures, increases correspondingly. If during this time interval the impulsive load dies down quickly enough, then the constant resistance (yield moment) may be adequate to prevent the attainment of the failure conditions.

This paper is concerned with the theoretical and experimental analysis of the behaviour of a ductile structure subjected to short-term impulsive loading beyond the elastic range, so that during a brief time interval it enters the labile state.

2. ELASTO-PLASTIC RESPONSE SPECTRA

2.1 Models, Definitions

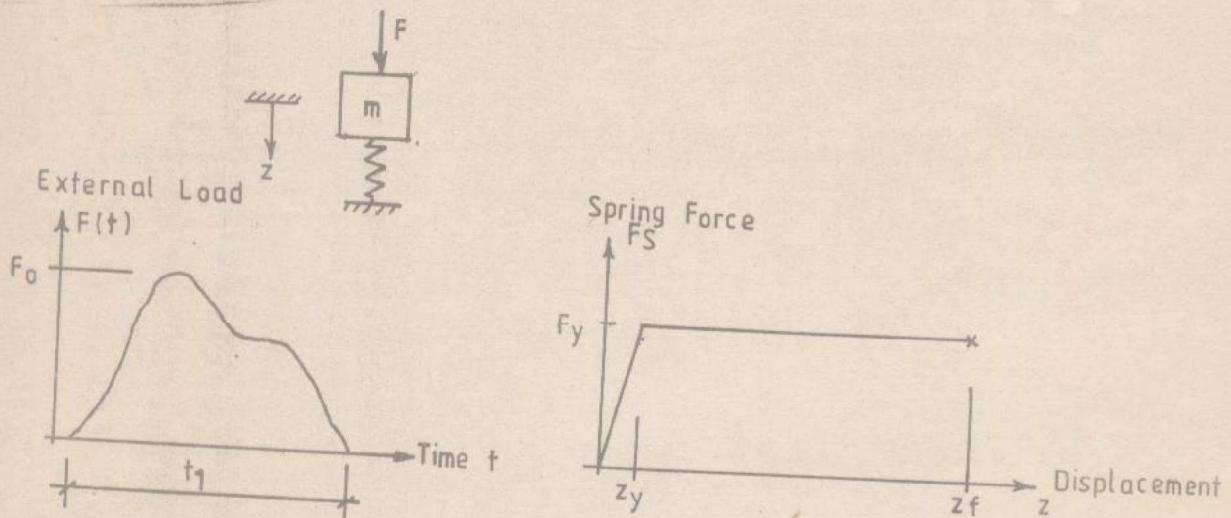


Figure 3: Model for the elasto-plastic single mass oscillator

The model for the calculation of elasto-plastic response spectra is the elasto-plastic single mass oscillator (fig.3). During the elastic phase, up to a maximum displacement z_y , the spring force is proportional to the displacement. After the critical displacement z_y is exceeded, the spring force remains constant at its maximum value of F_y , and the oscillator suffers plastic deformations. In the calculations, we obviously must differentiate between the two phases.

The general, impulsive load acting on the oscillator has two noteworthy quantities, namely the maximum value F_o and the duration t_1 . Two important parameters can be defined as:

$$\text{- The time ratio: } TR = \frac{\text{Load Duration}}{\text{Elastic Eigenperiod of the Oscillator}} = \frac{t_1}{T} \dots\dots\dots(2)$$

$$\text{- The load ratio: } LR = \frac{\text{Maximum Spring Force}}{\text{Maximum Value of the Impulsive Load}} = \frac{F_y}{F_o} \dots\dots\dots(3)$$

Also important is the time function or "shape" of the impulsive load, which can be described as:

$$\text{- } F(t) = F_o \cdot f(t) \dots\dots\dots(4)$$

where $f(t)$ is the time function (maximum value=1) of the load with maximum value F_o .

2.2 THE ELASTIC PHASE

During the primary, elastic phase, the equation of motion is given as:

$$- F_I + F_D + F_S = F(t) \quad \text{or} \quad \dots\dots(5)$$

$$- mz + cz + kz = F(t) \quad \text{where} \quad \dots\dots(6)$$

$$\left. \begin{aligned}
 F_I &= \text{Inertial Force} = \text{Mass} \times \text{Acceleration} = mx \\
 F_D &= \text{Damping Force} = \text{Damping Constant} \times \text{Velocity} = cz \\
 F_S &= \text{Spring Force} = \text{Spring Constant} \times \text{Displacement} = kz
 \end{aligned} \right\} \dots\dots(7)$$

In practice, damping plays only a minor role in the extreme structural reactions to short-duration loads, since several vibration cycles are required for its effects to be in full evidence. We shall therefore neglect damping in the following, thus simplifying the calculations.

The eigenperiod T of the oscillator can be calculated as:

$$- T = 2\pi \cdot \sqrt{m/k} \quad \dots\dots(8)$$

Many procedures are available for the numerical integration of Equation [6]. The one employed here assumes that the acceleration varies linearly during each time increment while the properties of the system remain constant during this time interval. According to [1], the increase $\Delta z(t)$ in the displacement during the time interval Δt is given as:

$$- \Delta z(t) = \frac{\Delta F(t)/k + (6/\Delta t) \cdot (m/k) \cdot z(t) + 3 \cdot (m/k) \cdot z(t)}{1 + (6/\Delta t^2) \cdot (m/k)} \dots\dots(9)$$

Using the relationship

$$- F_y = k \cdot z_y \dots\dots(10)$$

as well as Equations |4|, |5| and |8|, the equation |9| can be simplified to:

$$- \Delta z(t) = \frac{z_y}{LR} \cdot \Delta f(t) + \frac{6}{4\pi^2} \cdot \frac{T^2}{\Delta t} \cdot z(t) + \frac{3}{4} \cdot \frac{T^2}{4\pi^2} \cdot z(t) \dots\dots(11)$$

The displacement and the velocity at the time (t+ Δt) can be determined as:

$$- z(t+\Delta t) = z(t) + \Delta z(t) \dots\dots(12)$$

$$- z(t+\Delta t) = \frac{3\Delta z(t)}{\Delta t} - 2 \cdot z(t) - \frac{\Delta t}{2} \cdot z(t) \dots\dots(13)$$

Equations |5|, |7|, |8| and |10| can be used to determine the acceleration as:

In the usual case with starting from rest conditions:

$$- z(t+\Delta t) = \frac{4\pi^2}{T^2} \cdot z_y \cdot \left[\frac{f(t+\Delta t)}{LR} - \frac{z(t+\Delta t)}{z_y} \right] \dots(14)$$

In the usual case with starting from rest conditions:

$$- z(t = 0) = z(0) = z(0) = 0 \dots(15)$$

it can be shown that the displacements are always multiplied by z_y . Thus for the relationships of interest we can assume $z_y = 1$, without having to worry about errors in the desired results.

As a final hint, the time interval Δt should be less than about $T/10$, in order to avoid accumulation of errors.

2.3 The plastic Phase

If $z(t)$ always remains below z_y , then the structure remains fully elastic. If, however, z_y is attained or exceeded, then the spring force remains constant instead of increasing proportionally with the displacement, and Equation |6| can be modified into:

$$- mz(t) = F(t) - F_D = F(t) - F_y \dots(16)$$

or, taking Equations |4|, |5| and |8| into account as well:

$$- z(t) = \frac{4\pi^2}{T^2} \cdot z_y \cdot \left[\frac{f(T)}{LR} - 1 \right] \dots(17)$$

The acceleration increase over the time interval Δt can be calculated as the difference between the accelerations at the times $(t + \Delta t)$ and (t) :

$$- z(t) = z(t + \Delta t) - z(t) = \frac{4\pi^2}{T^2} \cdot z_y \cdot \left(\frac{f(t + \Delta t) - f(t)}{LR} \right) \dots (18)$$

Under the assumption that the acceleration changes linearly during the time interval Δt , it can be readily shown that:

$$- z(t + \Delta t) = z(t) + z(t) \cdot \Delta t + \Delta z(t) \cdot \Delta t / 2 \dots (19)$$

$$- z(t + \Delta t) = z(t) + z(t) \cdot \Delta t + z(t) \cdot \Delta t^2 / 2 + \Delta z(t) \cdot \Delta t^2 / 6 \dots (20)$$

The plastic phase can be considered to have ended, when the displacement is reduced for the first time, ie. when:

$$- z(t + \Delta t) < z(t) = z_p \dots (21)$$

The calculations during this relief stage should be done as for the elastic phase, using an appropriate function in order to determine the (falling) spring force F_s :

$$- F_s = k \cdot \left(z(t) + z_y - z_p \right) \dots (22)$$

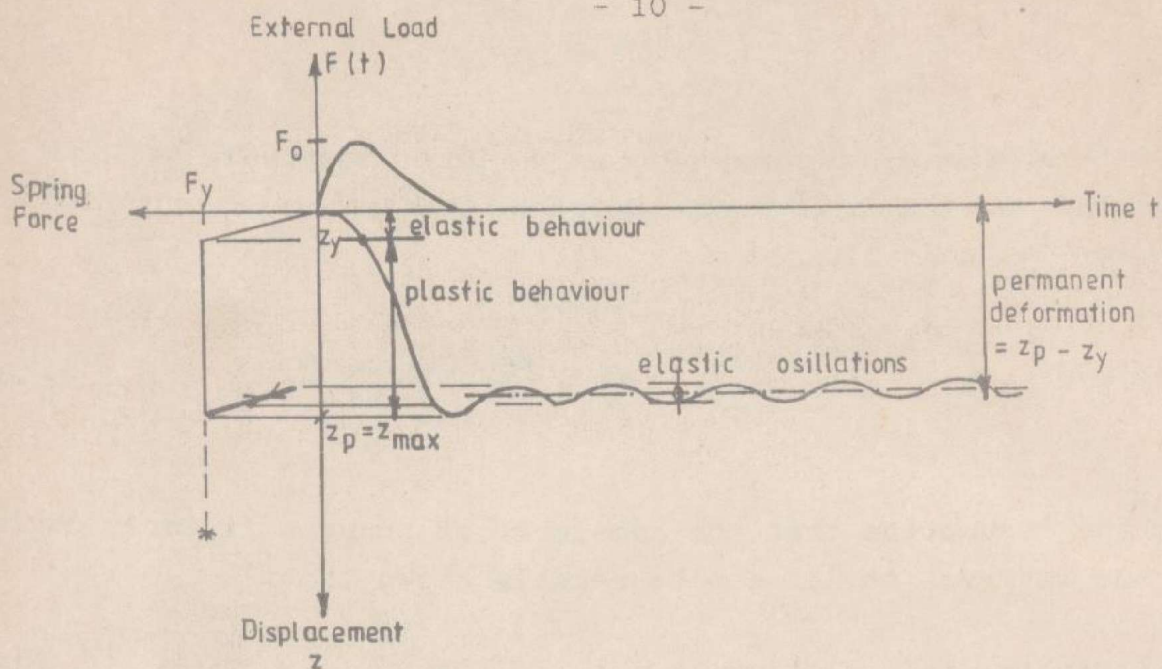


Fig. 4: Elastic and Plastic Phases of Vibration - typical case.

Fig. 4 shows the elastic and plastic phases of vibration. For the computer calculation, the transition from one phase to the next should be observed:

- (a) Initially, for $z(t) < z_y$: elastic phase.
- (b) If $z(t) > z_y$ and increasing: plastic phase.
- (c) If $z(t) > z_y$ and decreasing, eg. from z_p till $(z_p - z_y)$, as well as reloading up to z_p : elastic phase, but take account of the plastic deformations by replacing kz with $k[z(t) + z_y - z_p]$.

2.4 Results for a Sudden, Rectangular Impulsive Load

As an example, the calculation has been carried out for a

rectangular impulse, ie. a sudden load of constant magnitude F_0 , and of duration t_1 . For the practical calculation we should start by choosing parameters for the load ratio LR ($0 < (F_y/F_0 \leq 2)$) and the time ratio TR ($0 < t_1/T \leq 10$). The calculation is carried out as described above. The requisite ductility in order to avoid failure is the ratio of the maximum displacement obtained to the critical elastic limit for deformation:

$$\gamma = \frac{z_{\max}}{z_y} \quad \dots(23)$$

The calculation is repeated for several parameters of the load ratio LR and the time ratio TR. The results obtained are first sketched with the ductility γ as the abscissa, and the Load Ratio LR as ordinate: the Time Ratio TR is shown as a parameter (fig. 5).

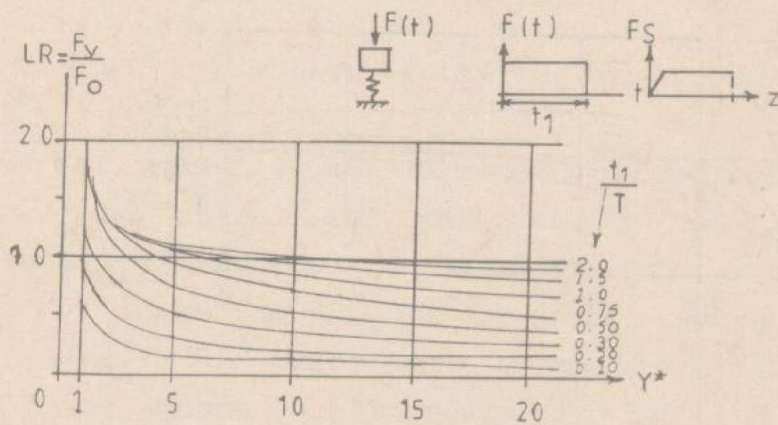


Fig. 5: Effective Load Ratio LR for a rectangular Impulsive Load: Primary plot of the results.

Based on this plot, a final, more distinct graph of the results can be prepared with the Time Ratio TR as abscissa, the Load Ratio LR as ordinate, and the ductility γ as parameter (fig. 6). Thus for a Time Ratio TR=0.5, for design purposes the maximum value of the impulsive load will have to be doubled for a brittle material ($\gamma = 1$) where no Plastic deformations are possible or permissible.

If plastic deformations are possible, however, then for a ductility factor of $\gamma = 8$ for example, the structure can be safely designed for only about 0.55 of the impulsive load.

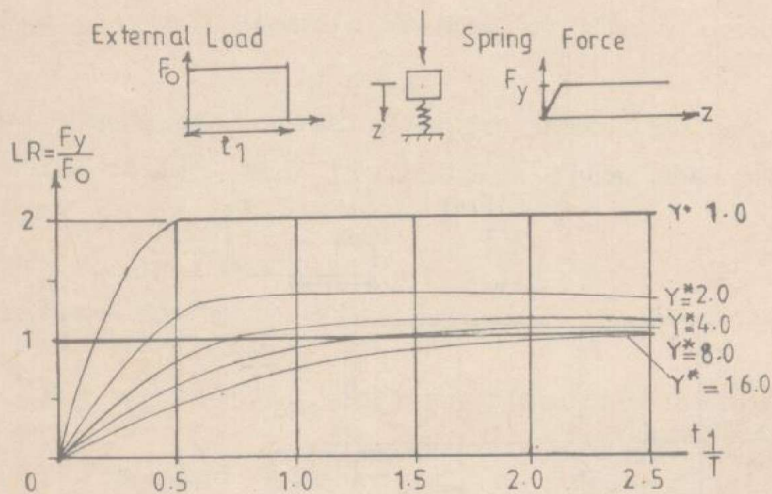


Fig. 6: Ductile material under a rectangular impulsive load: reduced load ratios, optimum presentation of the results.

3. PRACTICAL TESTS

3.1 Testing Installation

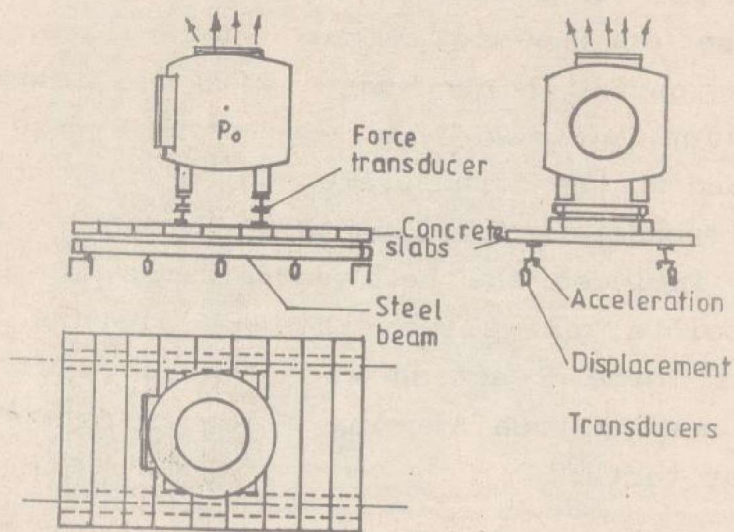


Fig. 7: Scheme of the testing installation

Two identical steel beams of span 8.15m resting on concrete abutments in an open field were used to test plastic behaviour under impulsive loading (fig. 7). The mass of these beams could be varied by placing on one or more layers of prefabricated concrete slabs. The slabs were 120mm thick, 640mm wide, and 3m long: a layer meant an increase in mass per beam of about 430kg/m'. The slabs were placed 10mm apart in order to avoid a stiffening of the structural system.

The load was induced with a vented dust explosion. The container in which the explosion took place had a volume of 10m^3 , a mass of 3.5t, and stood on the testing installation as shown in fig. 7. Two different dusts were used for the explosions, namely cellulose and aminophenazon. The top part of the container had an opening initially closed with a polyethylene foil, which was however blown away at an early stage of the explosion, thus releasing hot material from the container. In accordance with Isaac Newton's Law of Action and Reaction, venting leads to a recoil force which acts on the container and on the structure on which it is achored. Fig. 8 gives a visual impression of the tests performed. The most important measurements included the beam deflections at midspan and near the quarter points, as well as the gas pressure in the container. The recoil force F acting was calculated from the pressure $p(t)$ and the venting area A using a lienar relationship established from earlier tests:

$$- F(t) = 1.13 p(t) \cdot A \quad \dots(24)$$

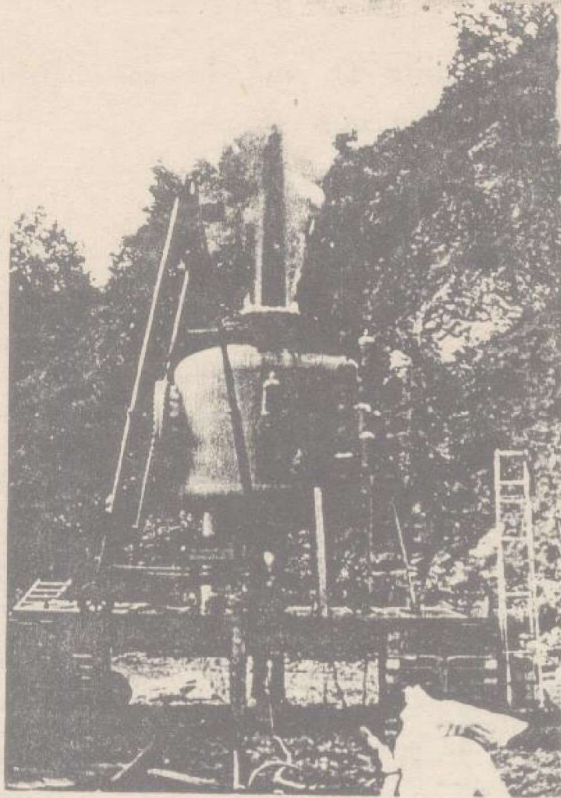


Fig. 8: Visual Impression of a vented Dust Explosion.

3.2 Hints regarding the Calculation Model for the Testing Installation

For comparison purposes with the actual measured values, calculations were made for the deformations of the testing installation under the recoil forces of the vented dust explosions. Essentially, the calculation was carried out per computer following the procedures described in Chapter 2 above. In this Chapter we are primarily concerned with how the actual beam structure was modelled as a single mass oscillator, in particular how the important items of generalized mass m^* , generalized stiffness k^* and generalized force $F^*(t)$ were obtained.

Under fully elastic conditions it was assumed that the beam would take on a constant vibration sinus-shape:

$$- \psi(x) = \sin(\pi x/L) \quad \dots(25)$$

According to [1] or [2], under this assumption the generalized properties of interest can be calculated as follows, where the quantities m , m_0 , and EI refer to the mass of the beam, the mass of the container, and the steel beam stiffness, respectively:

$$- m^* = \int^L m \cdot [\psi(x)]^2 dx + \sum m_i \cdot \psi_i = (mL/2) + m_0 \cdot [\sin \pi \alpha]^2 \dots(26)$$

$$- k^* = \int^L EI \cdot [\psi''(x)] dx = \pi^4 EI / 2l^3 \quad \dots(27)$$

$$- F^* = \sum f_i \cdot \psi_i = F(t) \cdot \sin \pi \alpha \quad \dots(28)$$

The calculation during the elastic phase was then carried out using these values as described in Chapter 2.2.

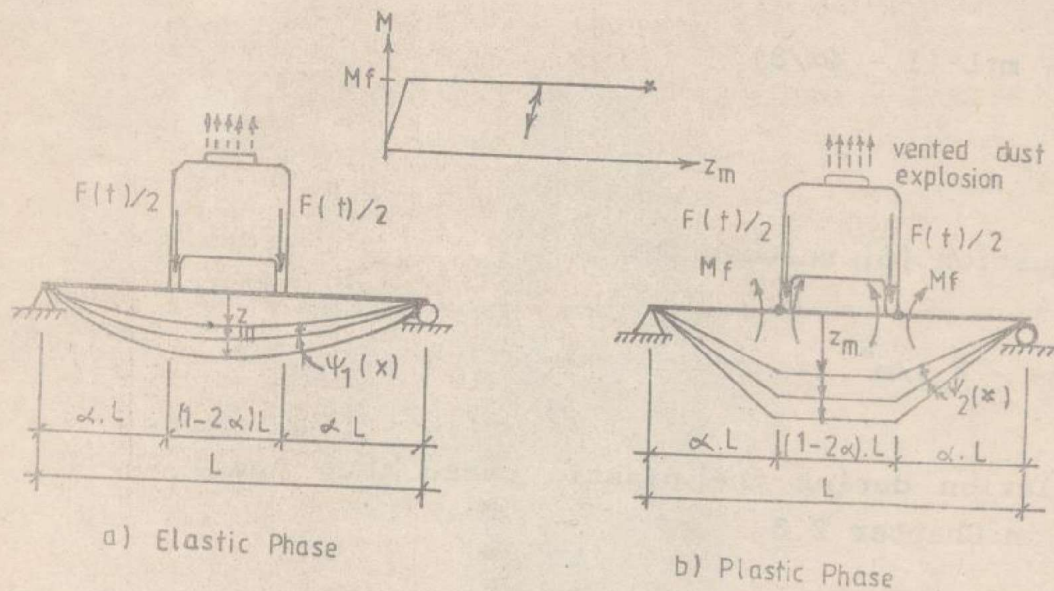


Fig. 9: Assumed Vibration Shapes of the Test Installation.

During the plastic hinges, thus new generalized properties - these depend upon the assumed vibration shape - had to be used. Fig. 9 shows the assumed vibration shapes during the elastic and plastic phases.

During the plastic phase it was assumed that due to the stiff container supports, no rotation was possible in the central part of the beam: instead, plastic hinges would form at two positions

below the container supports. Under the assumption that the beam vibration shape $\psi(x)$ remains practically linear between the supports and the plastic hinges, then it can be readily shown that the generalized properties during the plastic phase are:

$$- m^* = m_0 + m \cdot L \cdot (1 - 4\alpha/3) \quad \dots(29)$$

$$- F^* = F(t) \quad \dots(30)$$

so that Equation [6] reduces to:

$$- z = (F(t) - F_y) / m^* \quad \dots(31)$$

The calculation during the plastic phase thus could proceed as described in Chapter 2.3.

3.3 Experimental Results

The measurements showed that initially, the beams possessed a sinus-like vibration shape: the first, elastic edigenshape was activated, as expected. After a certain displacement was attained two plastic hinges were formed in the beam just below the container supports. The beam now possessed a different vibration shape, as predicted in Chapter 3.2. The attainment of this so called "labile state" will almost certainly lead to structural collapse in the case of long-duration loads: in our test, however, no collapse occurred because the impulsive load quickly died down before this could happen. After a maximum displacement the beams reverted back to the original, elastic vibration shape, and exhibited damped vibration about a new, lower displacement curve.

After the test a permanent deformation was observed, which corresponded to the beam shape during the plastic or yielding process (Fig. 10).

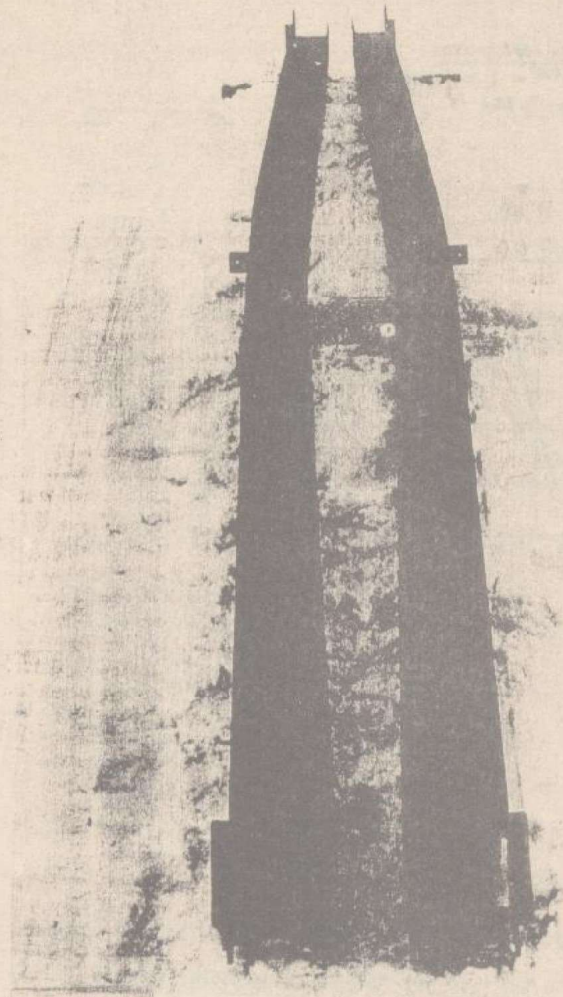


Fig. 10: Permanently deformed steel beams after loading tests with recoil e recoil forces of vented dust explosions.

In fig. 11 we see that the calculated displacements agreed quite well with the actual measurements.

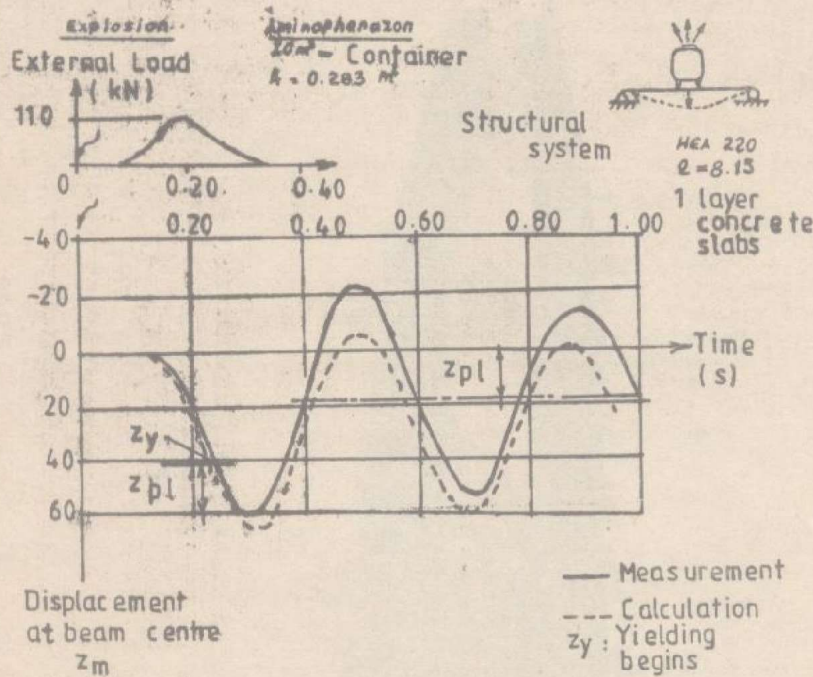


Fig. 11: Structural Behaviour in the plastic region - test results compared with the calculated behaviour.

According to the usual statical calculation with the ultimate moment M as collapse condition, the system depicted in fig. 11 - steel beams of type HEA220, span 8.15m, loaded with a layer of concrete slabs - could not have resisted a recoil force larger

than about 77kN. However, the actual maximum recoil force of 110kN was safely resisted with only 19mm permanent deformation at midspan. Even more impressive was the reserve in loading capacity observed in a repeated experiment with another, identical steel beam loaded with 2 concrete slab layers, ie. more mass. Statical estimates showed that the beam could not resist more than 35kN; however, the activated recoil force of again 110KN was safely resisted with only 33mm permanent deformation at midspan, which corresponds to a span/deformation ratio of 250:1.

4. CONCLUSIONS

In a series of tests, the structural behaviour during the transition from the elastic into the plastic phase was tested. The loading by the recoil forces of vented dust explosions resulted in so-called "plastic hinges" in the central part of the beam, so that during a short time period the simply supported beams entered the unstable labile state. This labile state, which is dreaded in normal statical, elastic analysis, did not lead to failure, however, because the mass of the structure slowed down the attainment of failure strains in the plastic hinges. After the short-duration load died down, the constant, plastic resistance M was able to stop any further strain development in the plastic hinges. The test results thereby confirmed the predictions of theoretical analysis. Thus a ductile material can be safely designed for reduced impulsive loads than those required by the usual elastic analysis. However, it should be borne in mind that in this case we should reckon with permanent deformations afterwards. In some cases this might result in undesired complications, for example compression members may buckle afterwards if they are permanently deformed by high moments induced by impulsive loads.

REFERENCES

- (1) R. Clough, J. Pensiën: "Dynamics of Structures", McGraw-Hill, Tokyo 1975.
- (2) M. Brunner: "Bauwerkbeanspruchungen durch die Ruckstosskräfte druckentlasteter Staubexplosionen" (Structural Loading induced by the Recoil Forces of vented Dust Explosions), Diss. ETH Nr. 7223, Zurich, 1983.

After graduating as Dip. Bauing. ETH-Z from the Swiss Federal Institute of Technology, Zurich, Switzerland, Dr. Brunner worked for 3 years in Switzerland as assistant. He obtained a doctorate in 1983 with a thesis on the impact loading induced by vented dust explosions. He worked in a Swiss consultancy office for another year before taking up appointment in 1985 at the University of Dar es Salaam. He is a member of the Institution of Engineers, Tanzania.